

Acoustic phonon quantization and low-frequency Raman spectra of spherical viruses

Mina Talati and Prafulla K. Jha

Computational Condensed Matter Physics Laboratory, Department of Physics, Faculty of Science, The M.S. University of Baroda, Vadodra, India 390 002

(Received 12 July 2005; revised manuscript received 23 September 2005; published 4 January 2006)

Low-frequency vibrational modes are calculated using elastic continuum approximation model for spherical viruses immersed in a medium. The blueshift in the vibrational modes is observed with decrease in the virus particle size. To incorporate the effect of surrounding environment, the anisotropic and finite medium is taken into account. The presence of medium significantly affects the Raman peaks representing acoustic modes and results into the linewidth broadening accompanied by damping of modes. The estimated damping constant and quality factor suggest less loss of energy of the fundamental breathing mode in the virus-glycerol configuration. The temperature effect on the virus results into the redshift of the low-frequency Raman peaks with increase in temperature. Significant differences in Raman spectra of wet and dry lysozyme are observed. The conformational changes are more prominent at low temperature for virus-water configuration suggesting that water works as a low energy barrier for conformational changes of spherical virus.

DOI: [10.1103/PhysRevE.73.011901](https://doi.org/10.1103/PhysRevE.73.011901)

PACS number(s): 87.64.-t, 63.22.+m, 61.46.-w, 62.30.+d

I. INTRODUCTION

Viruses and bacteria are one of the smallest living beings in nature and exist with a variety of shapes and sizes (diameter). However, most of the viruses are approximately spherelike in shapes with diameters in the range between nearly 20 nm and 100 nm. Many such nearly spherical viruses are revealed by x-ray crystallography to have icosahedral symmetry [1]. Typical viruses are miniscule pockets of proteins that contain a genetic material, RNA or DNA surrounded by a protein coat known as capsid. Viruses are mainly classified as RNA or DNA viruses, according to the type of nucleic acid forms their core. These nanometric viruses have found potential applications in diverse areas of rapidly developing nanotechnologies [2]. One of the most recent examples is the utilization of biological objects, such as viruses, as nanotemplates for the nanofabrication. For example, tobacco mosaic virus (TMV) and M13 bacteriophage have been utilized as biological templates in the synthesis of semiconductor and metallic nanowires [3,4]. Recently, genetically modified TMV and M13 viruses have been successfully used for the self-assembly of nanomaterials into liquid crystals, films and fibers [5]. It is expected that these genetically programmed viruses will contribute to the next generation of nanoelectronic circuits and optoelectronic devices. A confined nanometric biological system of a virus (virion) surrounded by a protein capsid is also of prime importance as excitations of their distinct vibrations could have applications in either diagnosis or treatment of the viral diseases. In addition, the knowledge of vibrational (acoustic phonon) modes of these viruses is important for material and structural characterization of the virus based nanotemplates.

Since these viruses have the diameters of the same order of magnitude as diameters of semiconductor nanocrystals or quantum dots, an analogy can be set for the elastic vibrations of the spherical viruses with those of the spherical quantum dots. The elastic vibrations of these spherical viruses should manifest themselves in the low-frequency Raman scattering spectra and therefore the interpretation of these spectra re-

quires the theoretical understanding of their low-frequency vibrational modes. As far as the estimation of vibrational frequencies in organic nanostructures (spherical virus particles) is concerned, there are only few reports so far [6,7]. The vibrational modes of viruses have been investigated by Babincová *et al.* [8] in context of the use of ultrasound in GHz for the destruction of HIV virus particles. Cooper *et al.* [9] have reported the acoustic oscillation for the detection of viruses. However, this is distinct from the excitation of the vibrational modes of the virus particle itself and occurs at much lower frequencies. Very recently, Balandin *et al.* [10] have reported the dispersion relations for the lowest vibrational frequencies of tobacco mosaic virus (TMV) and M13 bacteriophage immersed in air and water. Recently, Ford [6] has reported the theoretical estimates of vibrational frequencies of spherical virus particles by using two different approaches namely, the liquid drop model of Babincová *et al.* [8] and an elastic sphere model of Butalov *et al.* [11]. The investigations carried out by Ford [6] by using these approaches were able to give the frequency of the considered viruses but there was a difference of at least one order of the magnitude in their frequencies. Later on Saviot *et al.* [12] have corrected the errors appearing in the elastic sphere model approach used by Ford [6] and estimated a bit lower frequencies for the considered virus particles with $l=2$ (quadrupolar) modes. In this study their main emphasis was to show that the lowest frequencies are for $l=2$ and not for $l=0$ in contrast to the investigations of Ford [6]. Although they obtained correct values for the lowest vibrational mode, detailed and systematic investigations on the vibrational properties of the viruses are essential. Moreover, Saviot *et al.* [12] also emphasized for the calculation of damping of these phonon modes for embedded virus particles as they are grown or embedded in some medium. This will be useful to know if the sound waves can be used to detect and kill the viruses in proper virus-medium configuration. In recent years, the effect of various solvents (surrounding media) on the dynamics of proteins (viruses) has been a subject of active research as it is not only important for the fundamental

understanding of its working but also for its different applications [13,14]. Most of the studies mainly focus on the stability and biochemical activity of the proteins in different media, but so far, no attention has been paid to see the influence of different surrounding medium on the vibrations of the virus particles. The dynamics of vibrations in different medium is important to find a configuration to fulfill the objective of killing viruses by sending sound waves [6]. It has been shown by using Raman and neutron scattering of lysozyme that the protein dynamics is sensitive to their surrounding media namely, glycerol and trehalose [15–17].

In the present paper, some estimates of low-frequency vibrational modes of a spherical virus particle, under the framework of an elastic continuum model along with appropriate boundary conditions at the surface of a spherical virus, where a virus is treated as a uniform elastic sphere are reported. The symmetry of this model usually provides a series of good quantum numbers to identify the modes namely, the spheroidal and the torsional vibrational modes. The theoretical low-frequency (Raman or Brillouin) spectrum has also been calculated. It can be seen from study that there is a very good agreement between the frequency predicted from eigenvalue equation and peaks in the plots of Raman spectra. The effect of surrounding medium is clearly seen in the Raman spectra in terms of broadening of modes. Since the viruses are usually confined in some medium viz., water, air or any aqueous medium, to ensure specific function of the virus particle, the effect of surrounding medium on Raman spectrum is also studied. The damping time and damping constant have also been calculated for the nanoparticle modes in different medium. The paper is organized as follows: in Sec. II, we describe the methodology to obtain the low-frequency vibrational modes and spectrum; in Sec. III, we present results and discussion followed by the conclusion in Sec. IV.

II. METHODOLOGY

The set of discrete vibrational frequencies of a virus particle reflects its finite size, can be achieved using the elastic continuum approach under stress free boundary conditions at surface of virus particles. The vibrational modes of a nanometric virus particle are calculated by considering the acoustic vibrations of a particle as a whole from classical point of view, which was first given by Lamb [18] and later by Tamura *et al.* [19–21] and Saviot *et al.* [22,23] by considering different surrounding materials and thus various boundary conditions for the spherical elastic body of nanometer scale. This model has been quite successfully used for the description of phonons in several nanostructured systems by Murray *et al.* [23] and others [24–27].

Lamb's equation of motion for a three-dimensional elastic body in the differential form is given by the expression

$$\rho \frac{\partial^2 \vec{D}}{\partial t^2} = (\lambda + \mu) \vec{\nabla}(\vec{\nabla} \cdot \vec{D}) + \mu \nabla^2 \vec{D}, \quad (1)$$

where \vec{D} is a lattice displacement vector, the two parameters μ and λ are also known as Lamé's constants, and ρ is the mass density, which are related to the longitudinal and transverse sound velocities in bulk as

$$V_l = \sqrt{\frac{\mu}{\rho}} \quad \text{and} \quad V_t = \sqrt{\frac{2\mu + \lambda}{\rho}}. \quad (2)$$

The Lamé's constants λ and μ can be expressed in terms of elastic constants for an isotropic virus particle as $\lambda = 3K\sigma/(1+\sigma) = C_{12}$ and $\mu = \sqrt{Y/2(1+\sigma)}\rho = C_{44}$. Where σ , K , and Y are Poisson's ratio, modulus of rigidity, and Young's modulus, respectively. The energy eigenvalues for both spheroidal and torsional modes, for a spherical virus with radius R are obtained by using stress free boundary conditions in Eq. (1) at the surface of the spherical virus [28]. The eigenvalues of Eq. (1) for both spheroidal and torsional modes are described by orbital angular momentum quantum number l and harmonic n . Since the low-frequency Raman spectra is allowed only for the spheroidal modes ($l=0$ and 2), the eigenvalues for the spheroidal modes have been only estimated in the present study. Eigenvalue equation for spheroidal mode under stress free boundary conditions at the surface of the spherical nanometric body is obtained as [19]

$$2 \left\{ \eta^2 + (l-1) \left[l + 2 \left(\frac{\eta j_{l+1}(\eta)}{j_l(\eta)} - (l+1) \right) \right] \right\} \frac{\xi j_{l+1}(\xi)}{j_l(\xi)} - \frac{1}{2} \eta^4 + (l-1)(2l+1)\eta^2 + [\eta^2 - 2l(l-1)(l+2)] \frac{\eta j_{l+1}(\eta)}{j_l(\eta)} = 0, \quad (3)$$

where ξ and η are the dimensionless eigenvalues and relation between ξ and η is expressed as $\xi = \eta(V_t/V_l)$. The spheroidal mode is a vibration with dilatation and their eigenvalues depend on the materials through their longitudinal and transverse sound velocities. The eigenvalues ξ_l^s and η_l^s [29] are written as

$$\xi_l^s = \frac{\omega_l^s R}{V_l} \quad \text{and} \quad \eta_l^s = \frac{\omega_l^s R}{V_t}, \quad (4)$$

where ω_l^s is the angular frequency and R is the radius of an isolated spherical virus particle. The mode associated with $l=0$ and $n=0$ is called breathing mode. The $l=0$ and $l=2$ modes are Raman active according to the group theoretical analysis [30]. The $l=0$ mode is purely radial with spherical symmetry and produces totally polarized spectra, while $l=2$ mode is quadrupolar and produces partially depolarized spectra. The torsional mode is characterized as purely transverse mode, which is obtained from Eq. (1) and is defined for $l \geq 1$ [31]. The eigenvalues for $n=0$ for both spheroidal and torsional modes correspond to the surface modes while the eigenvalues ($n \geq 1$) correspond to inner modes.

By using the average sound velocities of the protein, the frequencies of the Raman lines corresponding to spheroidal modes can be estimated from Eq. (4). To get the low-frequency Raman spectra (intensity) with size of a spherical virus the methodology described by Murray *et al.* [32] and known as core shell model has been adopted. In this method, mean square displacement $\langle u^2 \rangle$ of the surface of the spherical virus is calculated and plotted against the frequency as the Raman scattering intensity depends on the square of the displacement. This approach has been used successfully for

TABLE I. The acoustic parameters for spherical virus embedded in surrounding medium.

	V_l (m/s)	V_t (m/s)	ρ (g/cm ³)	$\frac{\rho_m}{\rho_{\text{Virus}}}$
Water	1483	0	1.00	0.826
Virus	1817	915	1.21	1
Glycerol	1904	0	1.26	1.041

semiconductors and metals in glass matrix [25,29].

III. RESULTS AND DISCUSSION

Low-frequency vibrational modes of spherical virus particles immersed in a liquid medium are investigated by assuming the elastic properties of viruses close to the parameters of a protein crystal. The reported experimental values of longitudinal sound velocities of lysozyme, ribonuclease, and hemoglobin crystal are 1817 m/s [33], 1784 m/s [34], and 1828 m/s [34], respectively, which are quite close for these different protein crystals. It is assumed for the definiteness that the elastic parameters of viruses coincide with the parameters of lysozyme protein crystal from Ref. [33] and their values are summarized in Table I. A low-frequency analysis for spherical virus particles, calculated from the above-mentioned model, is presented here for a range of particle size and surrounding media. The energy eigenvalues for the spheroidal modes have been obtained for the spherical virus by solving Eq. (3) and presented in Table II along with the frequencies (Raman lines) for some harmonics n . Table II reveals that the lowest frequencies are for $l=2$ for all considered virus particle sizes. The blueshift of frequencies of the spheroidal modes with decrease in virus size as can also be observed from Table II, reveals the inverse relation of the frequency of the vibrations of a virus particle with size similar to that of a nanoparticle. The present paper also reports the calculated low-frequency Raman (Brillouin) spectrum for the free spherical viruses by using the methodology explained above which is presented in Fig. 1. The inverse re-

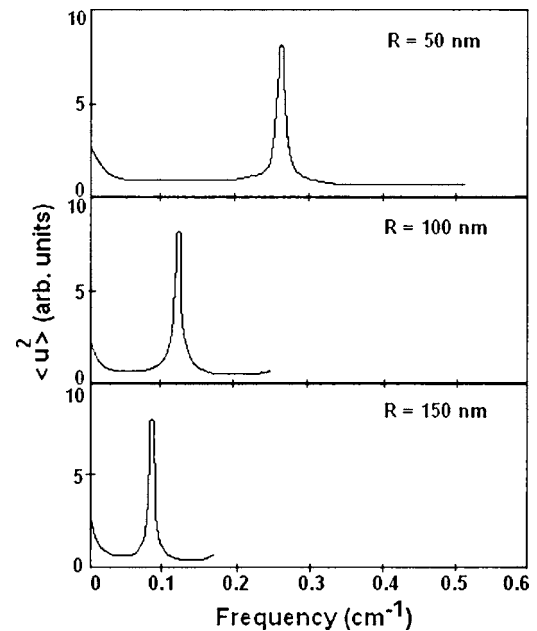


FIG. 1. Variations of low-frequency Raman peaks with the size of a spherical virus.

lation of size of a virus and frequency of a normal mode is observed similar to the frequency (Raman shift) calculated from the eigenvalue equation. It is also observed that there is in general good agreement between the Raman frequencies obtained by using these two methods. This also reveals the fact that a smaller virus particle scatters incident frequency (energy) more as compared to a bigger one in the low-frequency Raman scattering. Since the Raman scattering detects the fluctuations in the polarizability tensor α , the Raman scattering is related to the time variation of polarizability tensor of the virus particle. The polarizability tensor α is not a function of position, but is rather a property of the target object as a whole. Therefore, the polarizability tensor α oscillates at the same frequency as that of the mechanical vibrations of the virus particle. In the present consideration virus particle is a single elastic sphere embedded in an infinite matrix (medium) such as glycerol and water.

TABLE II. Eigenfrequencies (in cm⁻¹) of a spherical virus.

Eigenfrequencies (cm ⁻¹) of a spherical virus for spheroidal mode							
l	n	Eigenvalues	$d=20$ nm	$d=40$ nm	$d=60$ nm	$d=80$ nm	$d=100$ nm
0	0	5.400	2.618	1.309	0.872	0.654	0.523
	1	12.083	5.859	2.929	1.953	1.465	1.172
	2	18.411	8.928	4.464	2.976	2.232	1.785
1	0	3.586	1.739	0.869	0.579	0.434	0.347
	1	7.224	3.503	1.751	1.167	0.875	0.701
	2	8.457	4.101	2.050	1.367	1.023	0.820
2	0	2.650	1.285	0.642	0.428	0.321	0.257
	1	5.083	2.465	1.232	0.822	0.616	0.493
	2	8.612	4.176	2.088	1.392	1.044	0.835

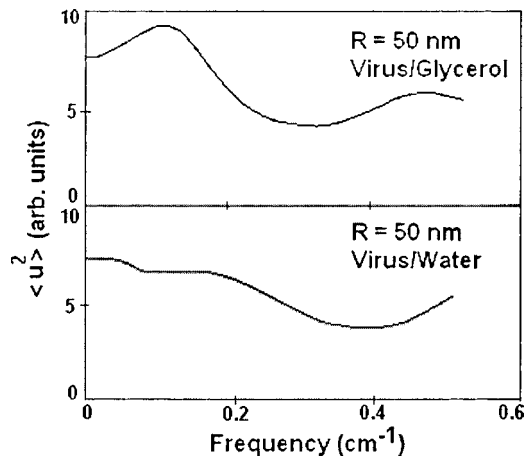


FIG. 2. Effect of matrix on low-frequency Raman peaks of a spherical virus.

Since the polarizability of virus particles depends on how tightly electrons are bound to the nuclei, it is a function of internuclear distances. In case of Raman active modes (symmetric stretch), strength of electron binding is different between minimum and maximum internuclear distances. This difference of strength of electron binding leads to changes in the polarizability during the vibrations and this vibrational mode scatters Raman light. The results on estimation of the vibrational modes especially, spheroidal modes of virus particles embedded in water or any other aqueous solutions are important, since this is the medium for the virus synthesis, purification and assembly processes. Water is also a strong IR absorbing medium, and generally, samples can be investigated more favorably by Raman rather than by Fourier transform infrared (FTIR) methods. Glycerol is generally regarded as one of the best biological cryopreservants [35].

The effect of water and glycerol media on low-frequency Raman peaks of virus is manifested in the linewidth broadening of Raman lines, which can be seen from Fig. 2. This broadening of peak approaching continuum in the spectra arises as a result of the mismatch in the acoustic parameters of the virus particle and surrounding medium as the low-frequency acoustic vibrations involve the whole system, the spherical virus and the medium. Another important feature, which is obvious from Fig. 2, is that the low-frequency Raman peaks for a virus-water system are more broadened than those for a virus-glycerol system. This could be because of the formation of stronger hydrogen bonds at the viral protein surface in case of polar water medium [36]. As the normal (lowest frequency breathing) mode in general is sharper and has longer lifetime due to high acoustic impedance mismatch at the surface in the virus-glycerol configuration (Fig. 2), the objective of destroying viruses by sending out sound waves is more probable in such a configuration [6]. This concept is based on the Rife therapy performed by a Rife frequency instrument, which destroys the microbe when there is a resonance between the mechanical oscillation frequency and microbe's lethal mechanical oscillation frequency [37].

To explain the effect of medium qualitatively in shifting and broadening of vibrational modes, specific acoustic impedance (Z_m) at the interface of the medium is introduced,

TABLE III. Damping time (ps) and quality factor (Q) for spherical virus of 50 nm radius.

Medium	Frequency (cm ⁻¹)	Damping time (ps)	Quality factor (Q)
Water	1.5393	17.3	0.7978
Glycerol	1.495	34.4	1.5447

which modifies Eq. (3) under the complex frequency approach [32]. The modified Eq. (3) for the lowest spheroidal mode can be expressed as

$$s^2 \tan(s) = \left[4 \left(\frac{V_{tp}}{V_{lp}} \right)^2 + is \left(\frac{Z_m}{V_{lp} \rho_p} \right) \right] [\tan(s) - s], \quad (5)$$

where V_{tp} , V_{lp} , and ρ_p are the transverse, longitudinal sound velocities, and density in virus particle. Here, $s = \omega R / V_{lp}$ and Z_m is the specific acoustic impedance at the interface of media which is simply density times the sound velocity for a plane interface, however, for a spherical interface it is a complex number given by $Z_m = \rho_m V_m [(k_m R)^2 - i(k_m R)] / [1 + (k_m R)^2]$, where ρ_m and V_m are the density and sound velocity in the surrounding matrix, respectively. Here, $k_m = \omega / V_m$ is the wave vector in surrounding medium. The modified energy eigenvalue is then used to evaluate the complex angular frequency ω , which can be further related with the damping time (τ_D) of the normal modes by using the expression $\tau_D = -1/\text{Im}(\omega)$. The damping time (τ_D) for a virus particle of 50 nm radius immersed in different media are presented in Table III. It is observed that the values of damping time for embedded virus particles are on the picoseconds time scale. Recently, Caliskan *et al.* [17] have also reported the picoseconds time scale for protein (lysozyme)-solvent coupling, which appears in both relaxations and low-frequency vibrations of protein. The quality factor is a quantity, which measures sharpness of the response of a resonating system to external excitation and can be expressed by using damping time, τ_D as $Q = \tau_D \omega$. The quality factor so obtained is presented in Table III for the spherical virus embedded in water and glycerol. It can be revealed from Table III that the quality factor Q is more for the virus embedded in the glycerol medium. This suggests that there is less loss of energy of the fundamental breathing mode in the virus-glycerol system. The energy losses, which determine Q for a particular mode, also determine the maximum amplitude of the oscillation when the resonance condition is exactly satisfied, as well as the width of the resonance (i.e., how far off the resonant frequency the system can be driven and still yield a significant oscillation amplitude).

Since the variation in temperature of a virus particle results into the variation in sound velocities [38], the effect of temperature on the frequency of the vibration is expected. Therefore, an effort has been made in the present study to investigate and understand this effect on low-frequency Raman spectra of a free virus and a virus-medium configuration. It is assumed in the present investigation that the change in transverse sound velocity of virus is negligible over considered (18–45) °C temperature range. The effect

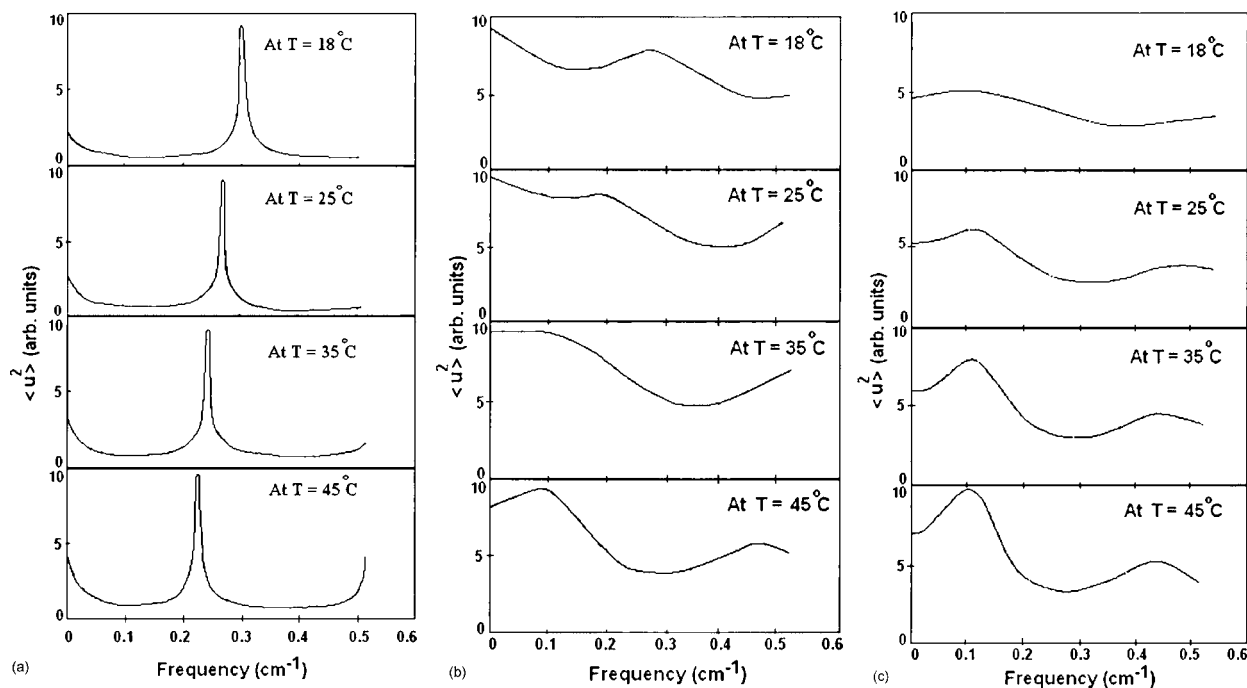


FIG. 3. Effect of temperature on low-frequency breathing mode of (a) a free virus ($R=50$ nm), (b) virus in water, and (c) virus in glycerol.

of temperature on virus particle has been incorporated in terms of its different longitudinal sound velocities for a spherical virus of size (diameter d) 100 nm. The temperature dependent longitudinal sound velocities of lysozyme in the present investigation are used from Ref. [38]. The temperature dependent low-frequency Raman spectra for a free spherical virus and an embedded virus in two different media such as glycerol and water are plotted in Fig. 3. The spectra of dry (higher temperature) and wet (lower temperature) spherical virus differ significantly, while the spectra of virus particle in water and in glycerol medium are qualitatively similar. This shows that the virus particles interact strongly with the environment. It is to be noted that the temperature effect for surrounding medium have not been considered due to nonavailability of the temperature-dependent sound velocities. Figure 3 reveals significantly that there are two effects of temperature on the low-frequency spectra of virus particles in water and glycerol, (1) there is a redshift (lower side) of Raman peak and (2) the broadening of the peak decreases with increase in temperature. While the former shows a known fact that the temperature variations of peak values (Raman shift) of a spherical virus follow variations of sound velocity [38] (i.e., elastic constant), the latter shows that the increase of temperature makes the virus particles dry and peaks become sharper due to the reduction of the coupling with the environment. Figure 4 presents the variation of the peak frequency (Raman shift) with the temperature for a free virus particle and virus particles embedded in water and glycerol. It is seen from Fig. 4 that the frequency decreases with the temperature for all cases. However, a remarkable feature is observed that the frequency falls sharply for the virus-water configuration at lower temperature and finally reaches close to the value of the virus-glycerol con-

figuration. This sharp fall of peak energy below a particular temperature in the case of the virus-water configuration may be because water works as a low energy barrier for conformational changes of virus to occur [38]. However, at higher temperature (above 30 °C) there are slight conformational changes with temperature for both configurations. This suggests that for the higher temperature, conformation slowly changes and the spherical virus (lysozyme) becomes more spherical as temperature is increased [39]. The temperature dependence of the low-frequency Raman spectrum calculated in the present paper is qualitatively similar to the Raman spectrum of lysozyme protein previously reported by Chalikian *et al.* [38].

IV. CONCLUSION

The present paper reports the quantization of acoustic phonon modes of a virus particle by using an elastic con-

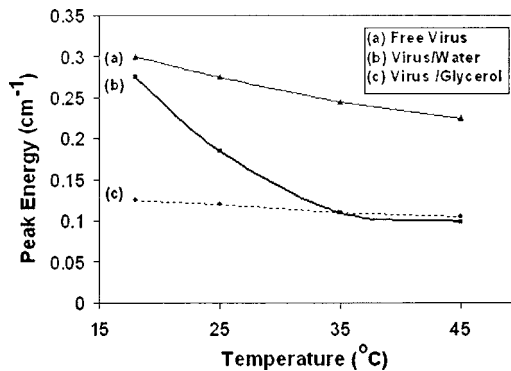


FIG. 4. Peak energy (cm^{-1}) vs temperature ($^{\circ}\text{C}$) for a spherical virus ($R=50$ nm).

tinuum model. Frequencies of spheroidal modes, low-frequency Raman (Brillouin) spectra, effect of water and glycerol on the breathing (low-frequency) mode have been estimated. The inverse size dependence of phonon frequency is obtained. The effect of surrounding medium is included in terms of acoustic mismatch under the framework of the complex frequency approach. The Raman peak is broadened due to damping when the virus is immersed in water than glycerol. The Raman peak sharpens in the case of glycerol or water. Therefore, the normal mode in the virus-glycerol configuration has longer lifetime and therefore this configuration has better probability for destroying the virus than the virus-water configurations. The damping time for embedded virus

is of the order of picoseconds. In addition, the broadening of the low-frequency Raman peak is explained on the basis of the hydrogen bond formation during the virus-medium coupling. The effect of temperature results into the redshift of the low-frequency spectra or spheroidal mode. The wet and dry virus spectra are significantly different.

ACKNOWLEDGMENTS

The financial assistance from the Department of Science and Technology and Department of Atomic Energy is highly appreciated. One of the authors (M.K.T.) is thankful to the CSIR, New Delhi for financial support.

-
- [1] R. Zandi, D. Reguera, R. F. Bruinsma, W. M. Gelbart, and J. Rudnick, *Proc. Natl. Acad. Sci. U.S.A.* **101**, 15556 (2004).
- [2] Q. A. Pankhurst, J. Connolly, S. K. Jones, and J. Dobson, *J. Phys. D* **36**, R167 (2003); J. Connolly and T. G. St. Pierre, *J. Magn. Magn. Mater.* **225**, 156 (2001).
- [3] W. Shenton, T. Douglas, M. Young, G. Stubbs, and S. Mann, *Adv. Mater. (Weinheim, Ger.)* **11**, 253 (1999).
- [4] M. Knez, A. M. Bittner, F. Boes, C. Wege, H. Jeske, E. Maiss, and K. Kern, *Nano Lett.* **3**, 1079 (2003); M. Knez, M. Sumser, A. M. Bittner, C. Wege, H. Jeske, T. P. Martin, and K. Kern, *Adv. Funct. Mater.* **14**, 116 (2004).
- [5] C. E. Flynn, S. W. Lee, B. R. Peelle, and A. M. Belcher, *Acta Mater.* **51**, 5867 (2003); C. Mao, D. J. Solis, B. D. Reiss, S. T. Kottmann, R. Y. Sweeney, A. Hayhurst, G. Georgiou, B. Iverson, and A. M. Belcher, *Science* **303**, 213 (2004).
- [6] L. H. Ford, *Phys. Rev. E* **67**, 051924 (2003).
- [7] Y. M. Sirenko, M. A. Stroschio, and K. W. Kim, *Phys. Rev. E* **53**, 1003 (1996).
- [8] M. Babincová, P. Sourivong, and P. Babinec, *Med. Hypotheses* **55**, 450 (2000).
- [9] M. A. Cooper, F. N. Dultsev, T. Minson, V. P. Ostanin, C. Abell, and D. Klenerman, *Nat. Biotechnol.* **19**, 833 (2001).
- [10] A. A. Balandin and V. A. Fonoberov, *J. Biomed. Nanotech.* **1**, 1 (2005).
- [11] V. L. Butalov, R. W. Grimes, and A. H. Harker, *Philos. Mag. Lett.* **77**, 267 (1998).
- [12] L. Saviot, D. B. Murray, A. Mermert, and E. Duval, *Phys. Rev. E* **69**, 023901 (2004).
- [13] K. B. Storey and J. M. Storey, *Sci. Am.* **263**, 92 (1990).
- [14] K. C. Fox, *Science* **267**, 1922 (1995).
- [15] G. Caliskan, A. Kisliuk, A. Tsai, C. Soles, and A. P. Sokolov, *J. Non-Cryst. Solids* **307**, 887 (2002).
- [16] G. Caliskan, A. Kisliuk, A. Tsai, C. Soles, and A. P. Sokolov, *J. Chem. Phys.* **118**, 4230 (2003).
- [17] G. Caliskan, D. Mechtani, J. H. Roh, A. Kisliuk, A. P. Sokolov, S. Azzam, M. T. Cicerone, S. Lin-Gibson, and I. Peral, *J. Chem. Phys.* **121**, 1978 (2004).
- [18] H. Lamb, *Proc. London Math. Soc.* **13**, 189 (1882).
- [19] A. Tamura, K. Higeta, and T. Ichinokawa, *J. Phys. C* **15**, 4975 (1982).
- [20] A. Tamura, K. Higeta, and T. Ichinokawa, *J. Phys. C* **16**, 1585 (1983).
- [21] A. Tamura and T. Ichinokawa, *J. Phys. C* **16**, 4779 (1983).
- [22] L. Saviot, B. Champagnon, E. Duval, and A. I. Ekimov, *Phys. Rev. B* **57**, 341 (1998).
- [23] L. Saviot, D. B. Murray, and M. del C. Marco de Lucas, *Phys. Rev. B* **69**, 113402 (2004).
- [24] A. Tanaka, S. Onari, and T. Arai, *Phys. Rev. B* **47**, 1237 (1993).
- [25] G. Scamarcio, V. Spagnolo, G. Ventruti, M. Lungarà, and G. C. Righini, *Phys. Rev. B* **53**, R10489 (1996).
- [26] N. N. Ovsiuk and V. N. Novikov, *Phys. Rev. B* **53**, 3113 (1996).
- [27] P. K. Jha and M. Talati, *Mater. Res. Soc. Symp. Proc.* **791**, Q8.11 (2003).
- [28] P. K. Jha and M. Talati, in *Focus in Condensed Matter Research*, edited by J. V. Chang (Nova, New York, in press).
- [29] M. Fujii, Y. Kanzawa, S. Hayashi, and K. Yamamoto, *Phys. Rev. B* **54**, R8373 (1996).
- [30] E. Duval, *Phys. Rev. B* **46**, 5795 (1992).
- [31] M. Talati and P. K. Jha, *Physica E* **28**, 171 (2005).
- [32] D. B. Murray and L. Saviot, *Phys. Rev. B* **69**, 094305 (2004); L. Saviot and D. B. Murray, *Phys. Status Solidi C* **1**, 2634 (2004).
- [33] M. Tachibana, K. Kojima, R. Ikuyama, Y. Kobayashi, and M. Ataka, *Chem. Phys. Lett.* **332**, 259 (2000).
- [34] C. Edwards, S. B. Palmer, P. Emsley, J. R. Helliwell, I. D. Glover, G. W. Harris, and D. S. Moss, *Acta Crystallogr., Sect. A: Found. Crystallogr.* **46**, 315 (1990).
- [35] J. Farrant, in *Current Trends in Cryobiology*, edited by A. U. Smith (Plenum, New York, 1970), p. 139; A. L. Tappel, in *Cryobiology*, edited by H. T. Meryman (Academic, London, 1966), p. 163.
- [36] S. B. Leslie, E. Israeli, B. Lighthart, J. H. Crowe, and L. M. Crowe, *Appl. Environ. Microbiol.* **61**, 3592 (1995).
- [37] G. Wade, <http://educate-yourself.org/gw>, Appendix B.
- [38] T. V. Chalikian, M. Totrov, R. Abagyan, and K. J. Breslauer, *J. Mol. Biol.* **260**, 588 (1996).
- [39] K. Monkos, *Current Topics in Biophysics* **25**, 75 (2001).